

Benzoxazoles as Selective Monoamine Oxidase B (MAO-B) Inhibitors

Vikram S. Sawant,^{†,‡} Hyeri Park,[†] Soo Yeon Paek,[†] Jieon Lee,^{†,‡} Ji Won Choi,[§] Ki Duk Park,[§] Kyung Il Choi,[†] Jihye Seong,^{†,‡,§} Sanghee Lee,^{†,*} and Hyunah Choo^{†,‡,*}

[†]Center for Neuro-Medicine, Brain Science Institute, Korea Institute of Science and Technology, Seoul 02792, Republic of Korea. *E-mail: slee19@kist.re.kr

[‡]Division of Bio-Medical Science and Technology, KIST School, Korea University of Science and Technology, Seoul 02792, Republic of Korea. *E-mail: hchoo@kist.re.kr

[§]Convergence Research Center for Diagnosis Treatment Care of Dementia, Korea Institute of Science and Technology, Seoul 02792, Republic of Korea

Received February 7, 2019, Accepted February 20, 2019

Keywords: Parkinson's disease, MAO-B, Selective inhibitor, Benzoxazole

Parkinson's disease (PD) is a central nervous system disorder accompanied by tremor, slow movement, motor impairment, and dementia.^{1,2} These symptoms of PD mainly result from the death of dopaminergic neurons in substantia nigra (SN) and the deficiency of dopamine inside the brain.³ Dopamine is a type of monoamine neurotransmitter and acts as a chemical messenger to regulate neuronal signaling in brain, thereby controls motor functions.⁴

Levodopa (L-dopa) is the major treatment for PD and exerts its effect as a dopamine precursor.⁵ However, dopa-resistance or serious complications are observed after an initial period of treatment.⁶ Besides L-dopa treatment, another therapeutic way to restore dopamine function is the suppression of dopamine catabolism. Monoamine oxidase (MAO) is involved in down-regulation of dopamine level which catalyzes the deamination and degradation of dopamine.⁷ Inhibition of MAO blocks the breakdown of dopamine, thereby prolongs the action of dopamine in the brain.⁸ There are two isoforms of MAO-A and MAO-B. Although they share about 70% of structure similarity, MAO-A and -B exhibit different substrate specificity as well as diverse regional distribution in brain tissue.⁹ MAO-B has been regarded as a therapeutic target for PD in clinic because the elevated activity of MAO-B was observed in the SN of PD patients.¹⁰

Currently, Selegiline and Rasagiline, both selective and irreversible MAO-B inhibitors, are used in clinics as a combination therapy with L-dopa (Figure 1).¹¹ Both drugs increased the amount of dopamine and efficiency of L-dopa.¹² However, severe adverse effects such as psychosis, headache, dizziness and nausea were reported due to neurotoxic metabolites.^{13,14} Recently, more potent and selective MAO-B inhibitor, Safinamide, was discovered as a reversible inhibitor (Figure 1).⁸ Safinamide also prevented neuronal cell death in animal models, improved motor function in clinical trials, and eventually was approved by FDA for mid- to late-stage of PD patients.¹⁵ All these evidences confirmed the importance of non-covalent inhibitor for MAO-B because the irreversibility induced short-lived actions of the inhibitors.¹⁶ Nevertheless, it

caused an adverse effect because of undesirable action as a sodium and calcium channel blocker.¹⁷ Therefore, the discovery of novel and selective MAO-B inhibitor with different molecular framework is still required.

Previously, we reported indole-substituted benzothiazoles and benzoxazoles as MAO-B inhibitors and demonstrated benzoxazole moiety working as a key pharmacophore for selective and reversible MAO-B inhibitor.¹⁸ Herein, we report piperidinyl- or pyrrolidinyl-substituted benzoxazole derivatives as potent and selective MAO-B inhibitors. We validated the reversible and competitive inhibitory effect of the title compounds on human MAO-B. We further investigated their binding modes against MAO-B via molecular modeling to elucidate binding interaction.

To examine the substituent effect of the cyclic amine functionality, we designed two classes of benzoxazoles with piperidinyl or pyrrolidinyl moiety at 5 or 6 position of benzoxazole, respectively. 5-Substituted benzoxazoles **4** were synthesized in three steps from 2-amino-4-bromophenol **1** (Scheme 1). 2-Amino-4-bromophenol **1** underwent cyclization by reaction with CH(OMe)₃ at 120 °C to produce 5-bromobenzoxazole **2** in 86% yield. 5-Bromobenzoxazole **2** was treated with NaO₂, SAR, Pd(OAc)₂, and Cu(OAc)₂ under acidic conditions to afford 2-aryl-5-bromobenzoxazoles **3** by palladium-catalyzed desulfurative C–H arylation.¹⁹ Buchwald-Hartwig cross coupling reactions of the compounds **3** with piperidine or pyrrolidine afforded the desired 5-substituted benzoxazoles **4** in approximately 23–72% yields.

6-Substituted benzoxazoles **7** were prepared starting from 5-bromo-2-nitrophenol **5** (Scheme 2). After reduction of 5-bromo-2-nitrophenol **5** using SnCl₂, the resulting 2-amino-5-bromophenol was directly converted into 6-bromobenzoxazole **6** by treatment with arylaldehyde followed by DDQ oxidation. The final 6-substituted benzoxazoles **7** were obtained in approximately 26–97% yields through Buchwald–Hartwig cross coupling reaction.

For structure–activity relationship (SAR) study, the biological effect of synthesized benzoxazoles on human

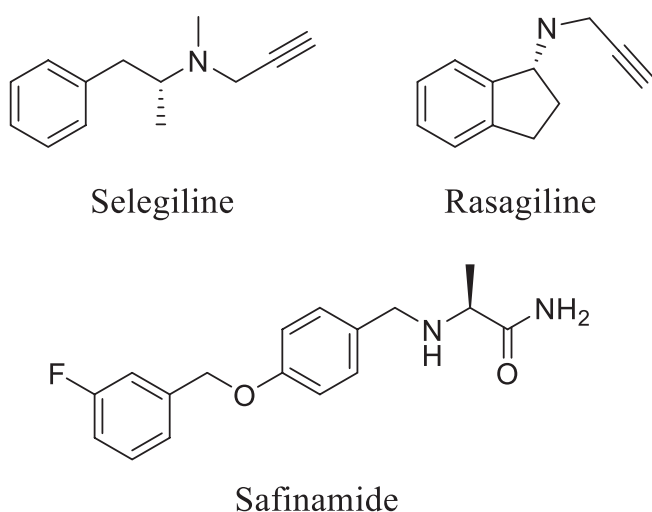
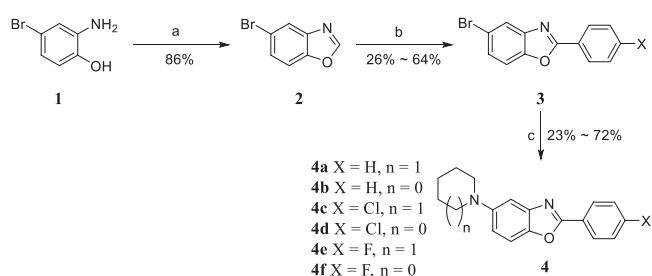
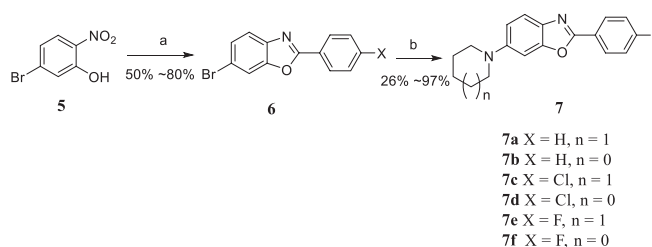


Figure 1. Structures of known MAO-B inhibitors.



Scheme 1. Synthesis of 5-substituted benzoxazoles **4**. Reagents and conditions: a) $\text{CH}(\text{OMe})_3$, 120°C ; b) NaO_2SAr , $\text{Pd}(\text{OAc})_2$, $\text{Cu}(\text{OAc})_2$, TFA, DME, 120°C ; c) amine, $\text{Pd}_2(\text{dba})_3$, BINAP, KO^tBu , toluene, 120°C or amines, $\text{Pd}(\text{OAc})_2$, BINAP, NaO^tBu , toluene, 120°C .

MAO-B (hMAO-B) was evaluated with Safinamide as a positive control. Since all the compounds, except **4c**, exhibited more than 50% of MAO-B inhibition at $10\ \mu\text{M}$ from initial test, they were subjected to determine IC_{50} values (Table 1). To confirm selectivity against MAO-A, we also measured their inhibitory effect against human MAO-A (hMAO-A) with clorgyline as a positive control and estimated the selectivity index. Similar to the potency, most of compounds also showed selectivity against MAO-A over 4- to 175-folds.



Scheme 2. Synthesis of 6-substituted benzoxazoles **7**. Reagents and conditions: a) i) SnCl_2 , EtOH, 70°C ; ii) ArCHO , MeOH, 50°C ; iii) DDQ, DCM, rt.; b) amine, $\text{Pd}_2(\text{dba})_2$, BINAP, KOTBu , toluene, 120°C .

Overall, compared to 5-substituted benzoxazole **4**, 6-substituted benzoxazole **7** showed enhanced potency with submicromolar IC_{50} 's (from 103 to 820 nM) that demonstrated an important role of 6-cyclic amine substitution in the benzoxazole moiety as a pharmacophore. In para-substitution on aryl moiety, replacement of X with fluorine, hydrogen, and chlorine roughly decreased their potency which implied that the size and electron withdrawing character on X were responsible for MAO-B inhibition. Particularly, fluorine substitution on aryl ring dramatically increased the selectivity index for MAO-A (**7e** and **7f**, 175-fold and 169-fold). The effect on piperidinyl or pyrrolidinyl substitution was somewhat complicated. It seemed to be associated with neighboring aryl group.

Based on all these SAR study, we identified the most potent and selective MAO-B inhibitor **7e** which proposed comparable inhibitory profile with Safinamide.¹⁸ As a result, **7e** was tested for further biological evaluation.

Inhibition of MAO-B by **7e** was further validated by the enzyme kinetic study, and the progress of reaction of MAO-B was monitored in the absence or presence of **7e**. By measuring the rate, we observed the saturated plateau in the level of reaction rate regardless of **7e** treatment. Analysis of Michaelis-Menten kinetics and Lineweaver-Burk plot revealed that V_{max} was unaffected with apparent shift in K_m upon inhibitor treatment. (Figure 2) These findings suggested that **7e** should compete with the substrate in the active site, which indicated the competitive inhibition of **7e** against MAO-B.

Since we verified **7e** as a competitive inhibitor working at the active site, further confirmation for the reversibility would be an important issue for therapeutic potential. Without any covalent warhead in chemical structure, we postulated **7e** as a reversible inhibitor. To confirm this hypothesis, we investigated the recovery of enzyme function after inhibitor treatments. Selegiline and Safinamide was used as irreversible and reversible control, respectively.^{20,21} Each hMAO-B enzyme reaction in the absence or presence of inhibitors was subjected to (1) MAO-B activity assay or (2) washout followed by re-testing for enzyme reaction.¹⁸ Compared to original enzyme activity (Figure 2), wash-off of enzyme-binding of **7e** or Safinamide induced the recovery of MAO-B catalytic function, resulting in showing that %-inhibitions after washout of **7e** and Safinamide were 83.50% and 76.00%, respectively, whereas Selegiline completely blocked the MAO-B even after washing step (Table 2). These results indicated **7e** as a reversible inhibitor for hMAO-B along with Safinamide.

To elucidate the binding mode between benzoxazole inhibitors and MAO-B, computational study was performed using co-crystal structure of hMAO-B and safinamide (PDB: 2V5Z).^{22,23} The most potent two benzoxazoles **7e** and **7f** were docked smoothly to the active site of hMAO-B. The orientation of the piperidine/pyrrolidine ring was positioned inside of the active site near to flavin adenine dinucleotide (FAD) and the fluoro-substituted phenyl group was positioned to the entrance of the binding pocket

Table 1. IC₅₀ value for hMAO-B and selectivity index against hMAO-A of benzoxazoles **4** and **7**.

Compd	X	n	MAO-B IC ₅₀ (nM) ^a	Selectivity index (SI) ^b
4a	H	1	501 ± 45	>19
4b	H	0	2724 ± 251	>4
4c	Cl	1	-- ^c	-- ^d
4d	Cl	0	4324 ± 800	>18
4e	F	1	700 ± 86	>25
4f	F	0	466 ± 85	>41
7a	H	1	656 ± 123	>31
7b	H	0	743 ± 260	>36
7c	Cl	1	820 ± 373	>44
7d	Cl	0	332 ± 89	>88
7e	F	1	103 ± 18	>175
7f	F	0	286 ± 53	>169
Safinamide			51 ± 1	>196

^a All of values were obtained by three independent experiments at least.

^b Selectivity index (SI) = IC₅₀ (hMAO-A)/IC₅₀ (hMAO-B). All of IC₅₀ values about hMAO-A postulated >10 000 nM due to low values of %-inhibition (under 28.6% at 10 μM).

^c Not determined.

^d Not calculated.

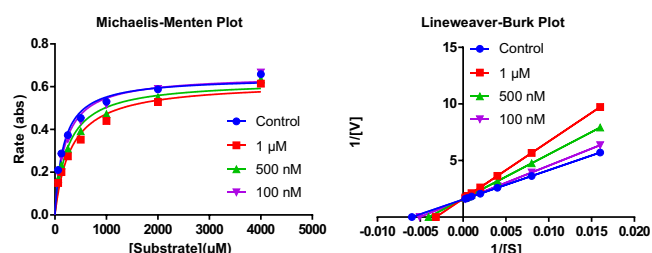


Figure 2. Validation of mechanism for MAO-B inhibition by **7e**. The reaction rates were measured at different concentrations of MAO-B substrate, benzylamine (0.0625, 0.125, 0.25, 0.5, 1, 2, and 4 mM) in absence or presence of **7e** with indicated concentrations.

(Figure 3). Major interactions of benzoxazole based on π -sulfur interactions with Cys172 and π - π interactions with Tyr326 revealed the importance of core structure. π -Donor hydrogen bonding between Pro104 and fluoro-substituted aryl group explained high potency of **7e** and **7f** by fluorine incorporation. On the other hand, carbon-hydrogen interaction between piperidine and Tyr435/Leu171 was detected only in **7e**, which distinguished the potency between **7e**

Table 2. Reversibility test of MAO-B inhibitor **7e**.

Inhibitor	%-Inhibition before washout ^a	%-Inhibition after washout ^a	Reversibility
7e	82.78	83.50	Reversible
Selegiline	100	0	Irreversible
Safinamide	95.69	76.00	Reversible

^a %-inhibition was normalized by control in absence of inhibitor. All enzyme reactions were performed with 1 μM of inhibitors and 100 mM of substrates.

and **7f**. Additional interaction with Ile199, Ile316, Gln206, and Leu171 provided extra stability to the complex by π -sigma, π -alkyl, and π -donor hydrogen bond interactions. According to the molecular docking study, various hydrophobic interactions described the molecular evidence for binding mode between **7e** and MAO-B.

The benzoxazoles with piperidine and pyrrolidine were synthesized and biologically evaluated as selective MAO-B inhibitors. Based on SAR analysis, we verified the importance of cyclic amine on 6-position and fluorine moiety on para-position of the aryl ring. Finally, we identified the most potent and selective compound **7e** among benzoxazole analogues with competitive inhibition and reversibility. Modeling study elucidated the structural understanding for binding mode between MAO-B and **7e** through various hydrophobic interaction. In conclusion, the novel selective and reversible MAO-B inhibitor **7e** was discovered, of which further study such as pharmacokinetic profiling or *in vivo* efficacy in animal model are in due course.

Experimental

Synthesis. **6-Bromo-2-(4-fluorophenyl)benzo[d]oxazole (6).** 5-Bromo-2-nitrophenol (500 mg, 2.29 mmol) was dissolved in ethanol (25 mL) and then tin(II) chloride dihydrate (2.59 g, 11.46 mmol) was added to this flask. The resulting mixture was stirred for 2 h at 70 °C. After the reaction was completed, the mixture was poured onto ice, neutralized to pH 7 with NaHCO₃, and extracted with EtOAc. The combined organic layers were dried over MgSO₄, filtered and evaporated. This compound was used for the next reaction without further purification. This compound (300 mg, 1.59 mmol) was dissolved in methanol (15 mL) and 4-fluorobenzaldehyde (0.156 mL, 1.59 mmol) was added to this solution. The reaction mixture was stirred at 50 °C for 12 h. After concentration, CH₂Cl₂ (10 mL) was added to the residue and the resulting solution was treated with DDQ (383 mg, 1.69 mmol). After stirring at room temperature for 30 min, the mixture was diluted with additional CH₂Cl₂ and washed with saturated Na₂CO₃. The organic layer was dried over MgSO₄. After evaporation, the crude compound was purified by silica gel column chromatography (ethyl acetate: hexane = 20:80) to obtain the desired product **6** (280 mg, 0.96 mmol) in 62.5% yield: ¹H NMR (400 MHz, CDCl₃) δ 8.24–8.22 (m, 2H), 7.75 (dd, *J* 1.6, 0.4 Hz, 1H), 7.62 (dd, *J* = 8.4, 0.4 Hz, 1H), 7.49 (dd, *J* = 8.4, 2.0 Hz, 1H), 7.24–7.20 (m, 2H).

2-(4-Fluorophenyl)-6-(piperidin-1-yl)benzo[d]oxazole (7e). Piperidine (0.95 mL, 9.6 mmol), Pd₂(dba)₃ (5 mg, 0.0048 mmol), BINAP (9 mg, 0.014 mmol) and KO^tBu (161 mg, 1.44 mmol) were added to a solution of 6-bromo-2-phenylbenzo[d]oxazole (140 mg, 0.48 mmol) in toluene (10 mL). The reaction mixture was stirred for 4 h at 120 °C. After cooling to room temperature, H₂O was added and then extracted with CH₂Cl₂. The organic solvent layers were dried over MgSO₄, filtered and evaporated. The residue was

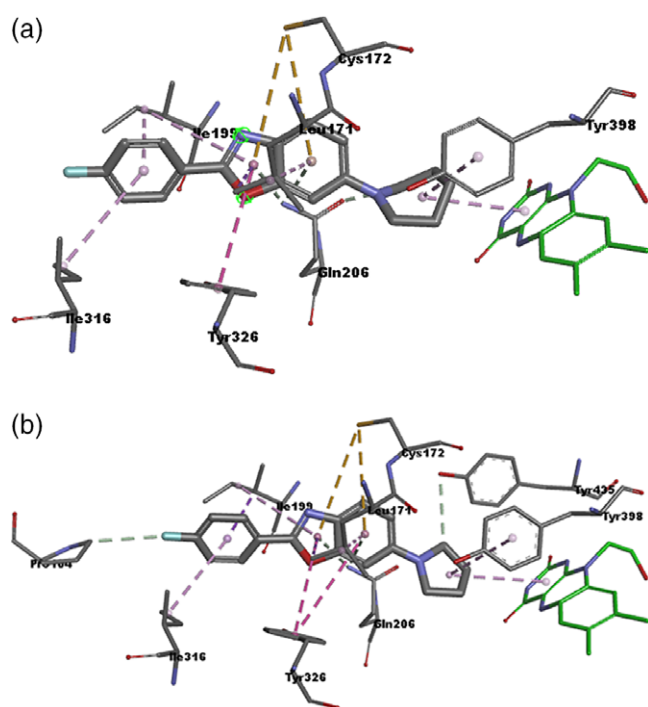


Figure 3. Molecular docking modes and two-dimensional schematic diagrams (inset) of (a) **7e** and (b) **7f** in the binding pocket of MAO-B.

purified by silica gel column chromatography (hexane: CH_2Cl_2 :ether=30:1:1) to obtain the desired product **7e** (32 mg, 0.107 mmol, 22.53%): ^1H NMR (400 MHz, CDCl_3) δ 8.20–8.16 (m, 2H), 7.58 (d, $J = 8.8$ Hz, 1H), 7.20–7.16 (m, 2H), 7.08 (d, $J = 2$ Hz, 1H), 7.01 (dd, $J = 8.8, 2.0$ Hz, 1H), 3.21 (t, $J = 5.4$ Hz, 4H), 1.78–1.73 (m, 4H), 1.63–1.58 (m, 2H); ^{13}C NMR (CDCl_3 , 100 MHz) δ 165.53, 163.13, 152.15, 151.28, 129.25, 129.16, 123.97, 123.94, 116.16, 115.94, 115.02, 97.96, 51.56, 25.86, 24.23; LC/MS (ESI $^+$): m/z : calcd for $\text{C}_{18}\text{H}_{17}\text{FN}_2\text{O}$: 296.35, $[\text{M}+\text{H}]^+$; found: 297.45.

MAO Enzyme Assay. Human recombinant MAO-A and MAO-B and substrates were obtained from Sigma-Aldrich (Darmstadt, Germany). Tyramine HCl and benzylamine HCl were used as MAO-A and MAO-B substrates, and sodium phosphate buffer (0.05 M, pH 7.4) was used in all reactions. The activity was measured by the production of H_2O_2 using resorufin via the Amplex Red $^{\text{®}}$ MAO assay kit (Invitrogen, Calsbad, CA, USA). Selegiline and Clorgyline for hMAO-B and hMAO-A were used as positive controls to validate experiments working. Briefly, 0.1 mL of phosphate buffer containing the inhibitors and hMAO-A or hMAO-B (0.5 μL , 71 U/mg) were incubated for 1 h at 37 $^{\circ}\text{C}$ in a 96-well plate. Then, the reaction started by adding of 200 μM Amplex Red $^{\text{®}}$ reagent, 1 U/mL horseradish peroxidase, and 1 mM tyramine HCl or benzylamine HCl as final concentrations in 0.2 mL as final volume. The consequent production of H_2O_2 was quantified using microplate reader (Molecular device) at 37 $^{\circ}\text{C}$ (abs; 570 nm). For

control experiments, appropriate dilutions of the vehicles were carried out. To exclude the signal noise from reagents or compounds, background absorbance was measured from the sample only without enzyme, then subtracted from original raw data. For analysis of kinetic experiment, GraphPad Prism was used to characterize enzyme reaction constants.

Acknowledgments. This research is supported by the Original Technology Research Program (NRF-2016M3C7A1904344) funded by the National Research Foundation of Korea (NRF). And this work is additionally funded by the Korea Institute of Science and Technology (KIST) Institutional Program (2E29190 and 2E29222).

References

1. T. M. Cutson, K. C. Laub, M. Schenkman, *Phys. Ther.* **1995**, *75*, 363.
2. A. Blochberger, S. Jones, *Clin. Pharm.* **2011**, *3*, 361.
3. D. C. German, K. Manaye, W. K. Smith, D. J. Woodward, C. B. Saper, *Ann. Neurol.* **1989**, *26*, 507.
4. G. Ayano, *J. Ment. Disord. Treat.* **2016**, *2*, 2.
5. J. E. Galvin, *Alzheimer Dis. Assoc. Disord.* **2006**, *20*, 302.
6. S. Chiba, E. Takada, M. Tadokoro, T. Taniguchi, K. Kadoyama, M. Takenokuchi, S. Kato, N. Suzuki, *Neurobiol. Aging* **2012**, *33*, 2491.
7. J. Meiser, D. Weindl, K. Hiller, *Cell Commun. Signal* **2013**, *11*, 1.
8. J. P. M. Finberg, J. M. Rabey, *Front. Pharmacol.* **2016**, *7*, 1.
9. C. W. Abell, W. Kwan, *Prog. Nucleic Acid Res. Mol. Biol.* **2000**, *65*, 129.
10. M. Chamoli, S. J. Chinta, J. K. Andersen, *J. Neural Transm.* **2018**, *125*, 1651.
11. P. Riederer, G. Laux, *Exp. Neurobiol.* **2011**, *20*, 1.
12. D. Robakis, S. Fahn, *CNS Drugs.* **2015**, *29*, 433.
13. P. Vezina, E. Mohr, D. Grimes, *Can. J. Neurol. Sci.* **1992**, *19*, 142.
14. L. Nayak, C. Henchcliffe, *Dis. Treat.* **2008**, *4*, 11.
15. S. Bette, D. S. Shpiner, C. Singer, H. Moore, *Ther. Clin. Risk Manag.* **2018**, *14*, 1737.
16. S. Jo, O. Yarishkin, Y. J. Hwang, Y. E. Chun, M. Park, D. H. Woo, J. Y. Bae, T. Kim, J. Lee, H. Chun, H. J. Park, D. Y. Lee, J. Hong, H. Y. Kim, S. J. Oh, S. J. Park, H. Lee, B. E. Yoon, Y. Kim, Y. Jeong, I. Shim, Y. C. Bae, J. Cho, N. W. Kowall, H. Ryu, E. Hwang, D. Kim, C. J. Lee, *Nat. Med.* **2014**, *20*, 886.
17. N. Malek, D. Grosset, *J. Exp. Pharmacol.* **2012**, *4*, 85.
18. M. H. Nam, M. Park, H. Park, Y. Kim, S. Yoon, V. S. Sawant, J. W. Choi, J. H. Park, K. D. Park, S. J. Min, C. J. Lee, H. Choo, *ACS Chem. Neurosci.* **2017**, *8*, 1519.
19. F. Zhao, Q. Tan, F. Xiao, S. Zhang, G. J. Deng, *Org. Lett.* **2013**, *15*, 1520.
20. K. Magyar, B. Szende, *Neurotoxicology* **2004**, *25*, 233.
21. T. Müller, *Clin. Pharmacol.* **2018**, *10*, 31.
22. C. Binda, J. Wang, L. Pisani, C. Caccia, A. Carotti, P. Salvati, D. E. Edmondson, A. Mattevi, *J. Med. Chem.* **2007**, *50*, 5848.
23. M. S. Nel, A. Petzer, J. P. Petzer, L. J. Legoabe, *Bioorg. Chem.* **2016**, *69*, 20.